ELSEVIER

Chemical Engineering Journal 80 (2000) 267–273

Chemical Engineering Journal

www.elsevier.com/locate/cej

Flow patterns in conical and cylindrical hydrocyclones

B. Chiné [a,1], F. Concha [b,*]

[a] *Faculty of Engineering, Catholic University of Concepción, Concepción, Chile*

[b] *Department of Metallurgical Engineering, Faculty of Engineering, University of Concepción, Casilla 53 C, Correo 3, Concepción, Chile*

Abstract

Using a two beam, 300 mW laser Doppler velocimeter, the tangential and axial velocity fields were determined for the water flow in a 102-mm modular hydrocyclone. The body of the equipment could be changed to transform it into a conical or a flat bottom hydrocyclone. During the tests the pressure drop and the diameter of apex and vortex were varied and the axial and the tangential velocities and their turbulence intensity were measured. The results shows that the inlet pressure affects only the magnitude of the velocities, but does not change the flow pattern. The tangential velocity is similar in both types of hydrocylones while the axial velocity is different. In both hydrocyclones the axial velocity is a function of the radial position but, while it is a linear function of the vertical coordinate in the cylindrical hydrocyclone, this is not the case for the conical vessel.

Keywords: Hydrocyclone; Laser Doppler velocimetry; Axial velocity; Tangential velocity; Turbulence intensity

1. Introduction

The conical hydrocyclone was first patented in 1891 by Bretney and thereafter became an important process unit in particle technology. Different hydrocyclone shapes were proposed, however only the conical and the cylindrical shape, have been applied industrially. The conical hydrocyclone is the most widespread dynamic classifier and the cylindrical vessel (flat bottom hydrocyclone) is used in a lesser extent, although there are important application as classifier or separator in a two-stage arrangement.

The flow inside a hydrocyclone is a three dimensional swirling flow confined in a cylindrical or conical geometry. The flow is a Rankine's vortex, that is, a combination of two vortices: (a) a forced vortex, or body rigid rotation, where the tangential velocity v_θ is proportional to the radius r ($v_\theta = k_1 r$); and (b) a free vortex or potential vortex, where the tangential velocity is inversely proportional to the radius ($v_\theta = k_2/r$). An axial movement directed to the bottom discharge and an axial reverse flow travelling to the vortex finder complete this flow pattern. The radial velocity in a hydrocyclone is small as stated by Bank and Gauvin [1] and confirmed by many workers.

The velocity profiles of conical hydrocyclones were measured first by Kelsall [2] and more recently a number of authors reported their measurements using laser Doppler velocimetry (LDV) (Fanglu and Wenzhen [3], Hsieh and Rajamani [4], Schummer et al. [5]). Only a few studies have been carried out to determine the flow pattern of cylindrical hydrocyclones. Baranov et al. [6] measured the tangential velocity in a counterflow hydrocyclone by the electrodiffusion method, while recently Chiné et al. [7] studied, by LDV, the flow in a cylindrical separator with peripheral discharge. Finally, no experimental data is available for cylindrical vessels with central bottom discharge.

It is the purpose of the present work to obtain a more detailed knowledge of the flow characteristics in conical and cylindrical hydrocyclones using the LDV technique, which permits a complete no-intrusive mapping of the flow field.

2. Experimental set up

2.1. Flow configuration

A 102-mm diameter modular Perspex hydrocyclone was used for the laser Doppler measurements. The body of the equipment could be transformed into a 625-mm high conical hydrocyclone or into a 310.5-mm high cylindrical hydrocyclone (see Fig. 1). In Table 1 the main dimensions of both hydrocyclones are given. For these models the overflow leaves the vessel through a 32 mm diameter vortex finder while apex diameter was 18 mm for the conical model and 19 mm for the flat bottom hydrocyclone.

* Corresponding author. Fax: +56-41-230759.
E-mail addresses: bchine@david.ucsc.cl (B. Chiné), fconcha@udec.cl (F. Concha).
[1] Fax: +56-41-481926.

1383-5866/00/$ – see front matter
PII: S1383-5866(00)00101-5

Nomenclature

β	included angle of the cone (rad)
Δp	pressure drop (psi)
D	hydrocyclone diameter (m)
D_O	vortex finder diameter (m)
D_U	apex diameter (m)
H	hydrocyclone height (m)
H_{CL}	height of the cylindrical section (m)
H_{CN}	height of the conical section (m)
I_θ	tangential turbulence intensity (%)
I_Z	axial turbulence intensity (%)
Q	feed flowrate (m^3/s)
Q_O	overflow rate (m^3/s)
Q_U	underflow rate (m^3/s)
r, θ, z	radial, azimuthal and axial coordinates
$r_{\theta,M}$	radial coordinate of $v_{\theta,M}$ (m)
$r_{z,0}$	radial coordinate where $v_z = 0$ (m)
R	radius of the hydrocyclone (m)
Re	Reynolds number
R_W	vortex finder external radio (m)
RMS_θ	root mean square value of v_θ (m/s)
RMS_Z	root mean square value of v_z (m/s)
S	swirl number
V	mean axial velocity (m/s)
V_{in}	inlet velocity (m/s)
$v_{\theta,M}$	maximum tangential velocity at a given z (m/s)
$v_{z,M}$	maximum overflow axial velocity at a given z (m/s)
$v_{z,m}$	maximum underflow axial velocity at a given z (m/s)
v_r, v_θ, v_z	velocity components in r, θ and z directions respectively (m/s)
ν	cinematic viscosity of water (m^2/s^2)

Water at room temperature (19–20°C) was fed to the model under controlled flow conditions. The hydrocyclones inlet was an involute tube with a 16×43-mm rectangular cross sectional area. This fluid was pumped from a 0.665-m^3 sump using a 4 HP pump and controlled by a set of valves. Feed pressure and flow rates were monitored with accurate manometers and rotameters. The discharged flow was measured by sampling volumes of fluid and recirculated.

Finally to generate tracer particles for the LDA measurements latex paintings particles were added to the fluid.

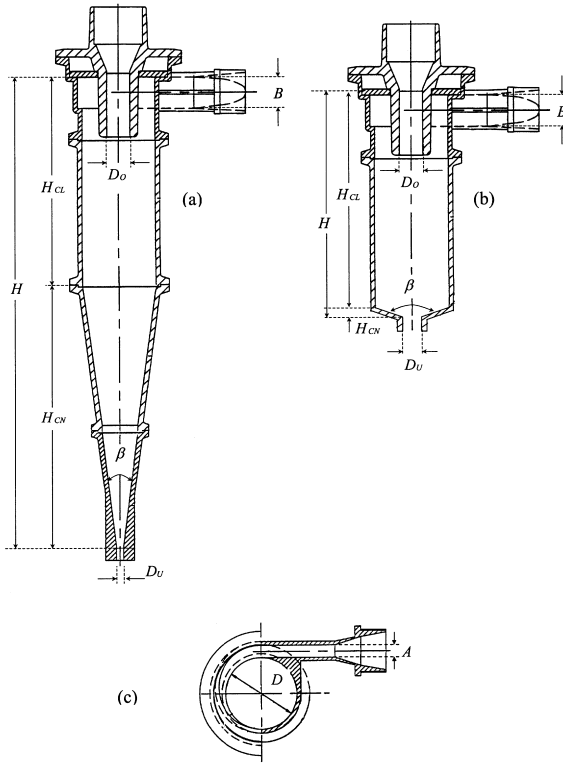

Fig. 1. Cross section of the hydrocyclone.

2.2. Measurement techniques

The velocity measurements inside the hydrocyclones were carried out using a two component laser Doppler velocimeter. To minimise the optical refraction of the laser beams at the curved hydrocyclone walls, the hydrocyclone model was immersed in a water filled jacket.

Coherent light with wavelength in the range 457–514.5 nm was directed to a transmitter box from a 300-mW argon-ion laser, where frequency shifting (see Durst et al. [8]) and colour separation was performed. A Bragg cell splits the light into two beams with a 40 MHz frequency shifting. These beams then pass through a dispersion prism, which provides two green (514.5 nm) and two blue (488 nm) light beams. The beams are led through fibre optic cables to a probe with a 160-mm focal length lens, which causes the four beams to intersect. Finally the collected back-scattered light is separated into green and blue components and is directed onto two photomultipliers. The Doppler signals were processed in two Burst Spectrum

Table 1
Dimensions of the hydrocyclones used in the experimental work[a]

	D (mm)	AxB (mm)	H_{CL} (mm)	H_{CN} (mm)	H (mm)	D_O (mm)	D_U (mm)	D_O/D_U	β (°)
Conical hydrocyclone	102	16×43	291	334	625	32	18	1.78	14
Cylindrical hydrocyclone	102	16×43	301	9.5	310.5	32	19	1.68	154

[a]See also Fig. 1 for a graphic illustration of the dimensions.

Table 2
Operating conditions

	Δp (psi)	V_{in} (m/s)	Q (m^3/s)	Q_O (m^3/s)	Q_U (m^3/s)	Q_U/Q_O	Re	S
Conical hydrocyclone	4	2.40	1.65×10^{-3}	1.30×10^{-3}	0.35×10^{-3}	0.269	2.06×10^{4}	4.00
	6.5	3.13	2.15×10^{-3}	1.87×10^{-3}	0.28×10^{-3}	0.149	2.6×10^{4}	4.12
	9	3.63	2.50×10^{-3}	2.32×10^{-3}	0.18×10^{-3}	0.077	3.12×10^{4}	4.21
Cylindrical hydrocyclone	4	2.06	1.42×10^{-3}	1.27×10^{-3}	0.15×10^{-3}	0.118	1.77×10^{4}	4.13
	6.5	2.75	1.89×10^{-3}	1.76×10^{-3}	0.13×10^{-3}	0.074	2.36×10^{4}	4.14
	9	3.26	2.24×10^{-3}	2.11×10^{-3}	0.13×10^{-3}	0.062	2.80×10^{4}	4.23

Analysers with fast Fourier transform to extract the Doppler frequencies. The experimental data were transferred to a computer for processing via an IEEE-488 interface.

During the measurements the probe was moved using a highly accurate three component (x–y–z) traverse system controlled by a computer via an RS-232 interface.

Velocity data were measured on four symmetrical vertical positions chosen on the curved walls (azimuthal coordinates θ=0, 90, 180, 270°). Being r and z the radial and axial coordinate respectively, the laser beams were focused on a median vertical r, z halfplane crossing the model, one for each azimuthal coordinate θ. On the median vertical plane, thirteen and six vertical z measurement levels were chosen for the conical and flat bottom hydrocyclone, respectively. For a given z coordinate, the first measurement point was placed near the wall of the cyclone and

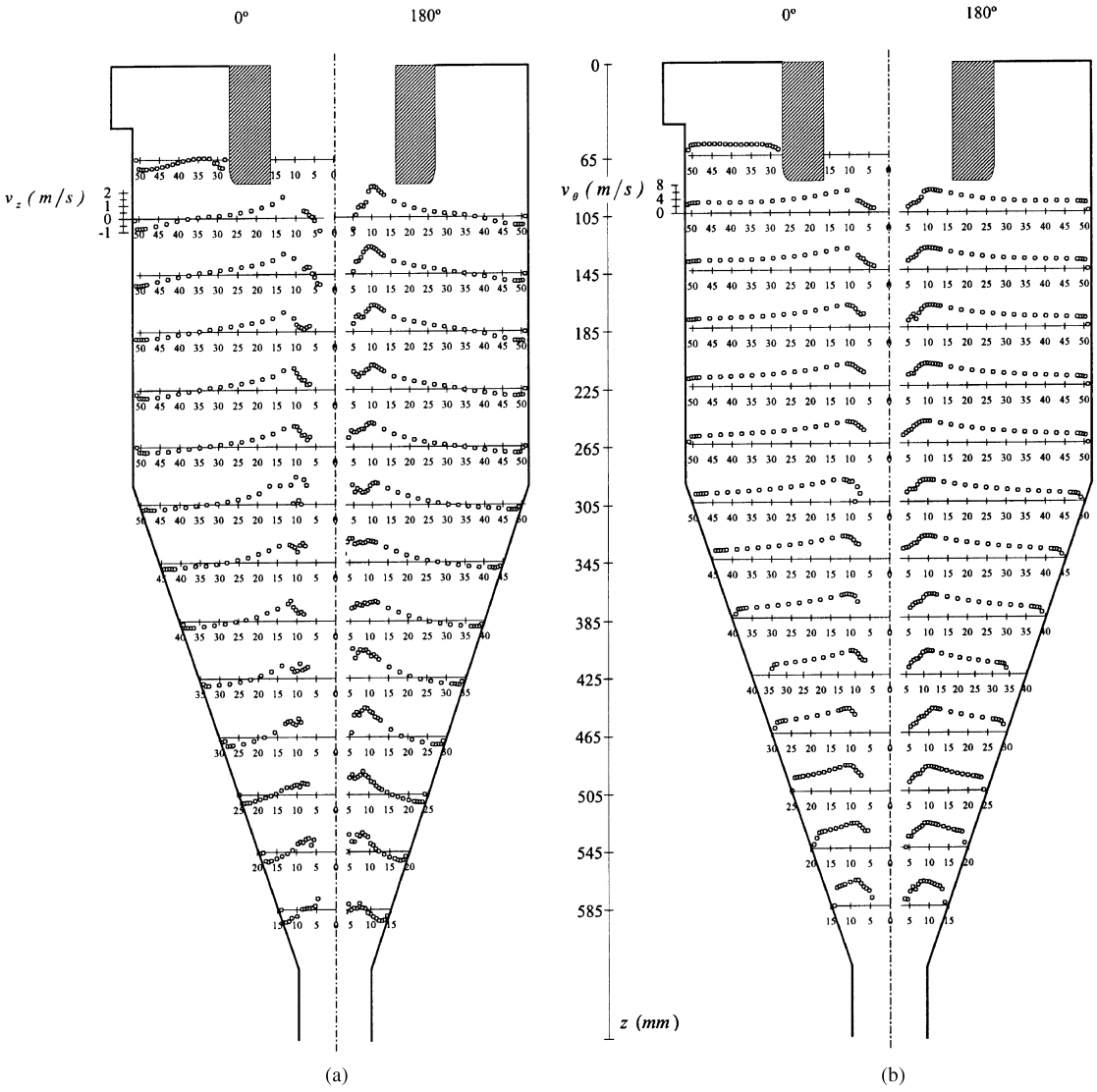

Fig. 2. Velocity profiles in the conical hydrocyclone.

the last point was chosen in proximity of the air core. A uniform measurement axial step Δz equal to 40 mm and radial steps Δr of 2.7 mm and 0.675 mm were applied. Finally, in all the experimental work a sample of typically 1000 Doppler bursts was taken for each measurement point.

2.3. Experimental procedure

The measurements were carried out at three feed pressure values (4, 6.5 and 9 psi). For both hydrocyclones the operating conditions are given in Table 2, where Δp, V_{in}, Q, Q_O, Q_U are the pressure drop, the inlet velocity, the feed flowrate, the over flowrate and the under flowrate, respectively. In the same table, $Re = VD/\nu$ represents the Reynolds number, V is the mean axial velocity in the hydrocyclone ($V = 4Q/\pi D^2$), D is the hydrocyclone diameter and ν is the water cinematic viscosity. To quantify the vortex intensity in the hydrocyclone, the swirl number $S = \int_{R_W}^{D/2} r^2 v_\theta v_z dr / \frac{D}{2}\int_{R_W}^{D/2} r v_z^2 dr$ was used, where R_W is the vortex finder external radio, v_θ is the tangential velocity and v_z is the axial velocity. Numerical computation of S was made using an integration interval equal to the experimental measurement step. The values of v_θ and v_z used in the computation are velocity data measured above the vortex finder entry region for z=65 mm. The final value of S is the mean of the values calculated for θ=0, 90. 270°.

3. Results

For a pressure drop of 6.5 psi, Fig. 2a and b and Fig. 3a and b give the experimental velocity profiles for the conical hydrocyclone and the cylindrical hydrocyclone respectively. The experimental results show that in both hydrocyclones the flow is approximately a forced vortex near the air core and a free vortex in the region between the maximum of tangential velocity v_θ and the solid wall. There are two opposite axial flows separated by a surface (*mantle*) where the axial velocity v_z is zero. Following the hydrocyclone geometry, the *mantle* describes a cylinder in the flat bottom vessel and in the cylindrical section of the conical vessel, while in the lower region of the conical hydrocyclone it is a conical surface.

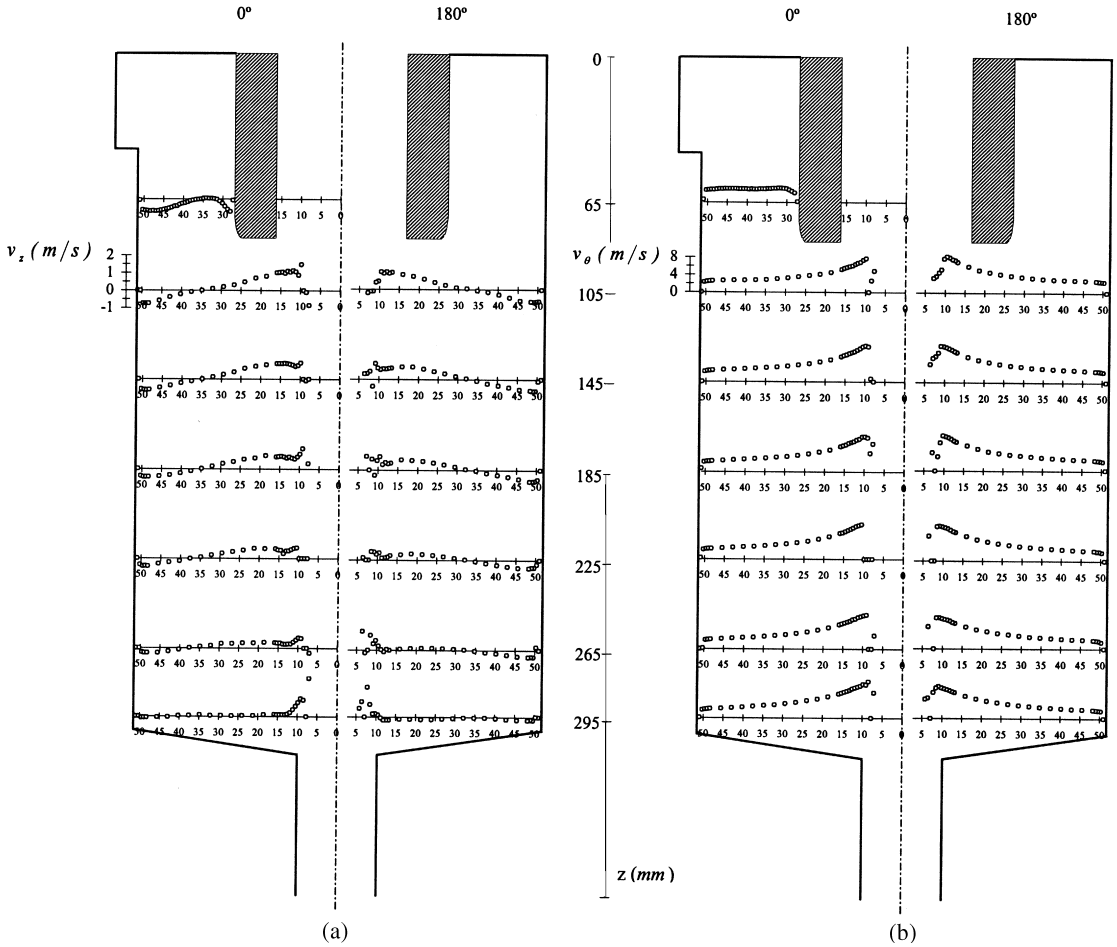

Fig. 3. Velocity profiles in the cylindrical hydrocyclone.

The velocity profiles are axisymmetric with exception of the profiles near the apex discharge and the air core, as the measurements for the halfplanes at θ=0, 90, 180, 270° have demonstrated. The LDV data obtained for Δp equal to 4 and 9 psi (not showed in this work) have proved that the flow does not depend on feed pressure, since the flow changes only its magnitude, while the velocity and the turbulence profiles maintain a constant pattern. The turbulence is neither homogenous nor isotropic, since the RMS values of v_z are always greater than RMS values of v_θ, except near the air core where they are of the same magnitude.

Other experimental tests were developed for the same hydrocyclones varying vortex finder and apex diameters (see Chiné [9]). Because of similar velocity and turbulence fields were obtained, their results will be not analysed.

3.1. Flow in the conical hydrocyclone

For the θ=90° halfplane of the conical hydrocyclone, the maximum overflow axial velocity $v_{z,M}$ increases with Δp for a given z coordinate and, when the pressure drop is maintained constant, decreases if z increases (Fig. 4a). The maximum tangential velocity $v_{\theta,M}$ grows with Δp and decays with z up to the cylinder-cone intersection and then increases near the apex (Fig. 4b). The coordinate $r_{\theta,M}$ of $v_{\theta,M}$ is not constant along the hydrocyclone and it depends on the feed pressure. The LDV data indicate (Fig. 4c) that

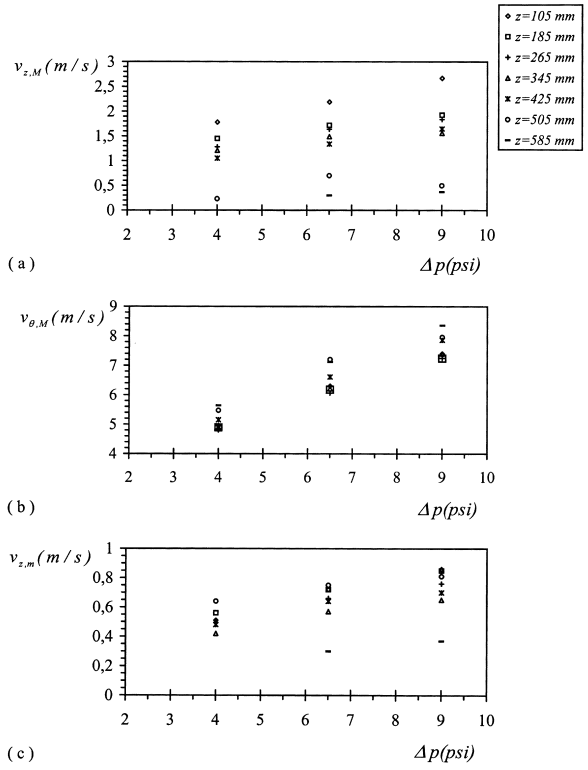

Fig. 4. Values of maximum overflow axial velocity, maximum tangential velocity and maximum underflow axial velocity in the conical hydrocyclone.

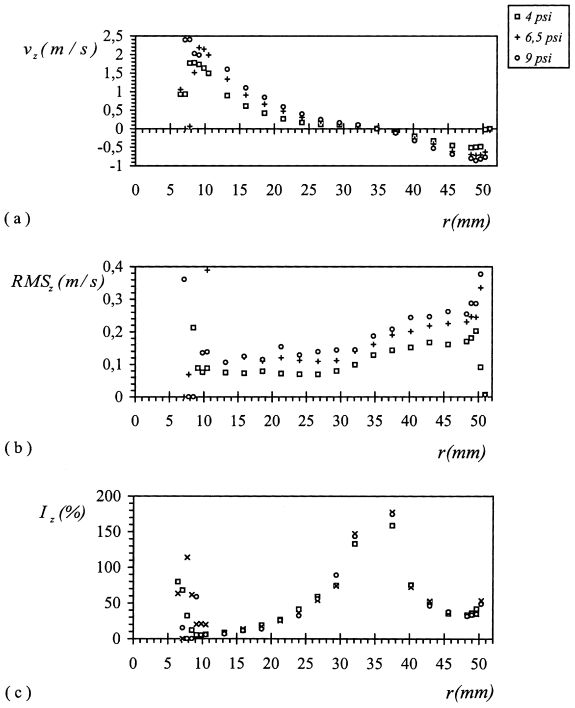

Fig. 5. Values of axial velocity in the conical hydrocyclone: mean velocity, RMS values and turbulence intensity.

the maximum underflow axial velocity $v_{z,m}$ increases with Δp and decrease with z, but starting at $z/H = 0.68$ it grows denoting an acceleration of the fluid flowing to the apex. The radial position $r_{z,0}$, where $v_z = 0$, does not change with Δp and its values is in the interval $0.61 \leq r_{z,0}/R(z) \leq 0.67$, where $R(z)$ is the radius of the cone at z.

A similar pattern has been found on the other halfplanes, although some appreciable variations of $r_{\theta,M}$ and $r_{z,0}$ shows the existence of asymmetry in the flow.

In Fig. 5a–c the values of v_z, its RMS values and the intensity of turbulence are plotted for z=105 mm, θ=90° and Δp=4, 6, 5, 9 psi. As it was said before, we observe only a change of magnitude in the profiles. Fig. 5b indicates that the axial velocity fluctuations are not homogenous, since they are greater near the wall and near the air core. The intensity of axial turbulence has a maximum at $v_z = 0$ and does not vary with Δp. For the same values of z, θ and Δp, the Fig. 6a–c give the mean values, RMS values and intensity of turbulence for the v_θ component. We can appreciate that v_θ, $r_{\theta,M}$ and RMS_θ changes with Δp while I_θ is approximately constant. In the same manner as v_z, the v_θ component presents greater fluctuations near the solid wall and near the air–liquid interface, but I_θ is one order of magnitude lower than I_z. As the fluid approaches the apex, the RMS_z and the RMS_θ increase.

The velocity profiles thus confirm a flow pattern made of an external quasi-potential vortex followed by an inner rigid body rotation where turbulence is higher. The surface that separates the two opposite axial flows is also characterised by a higher turbulence.

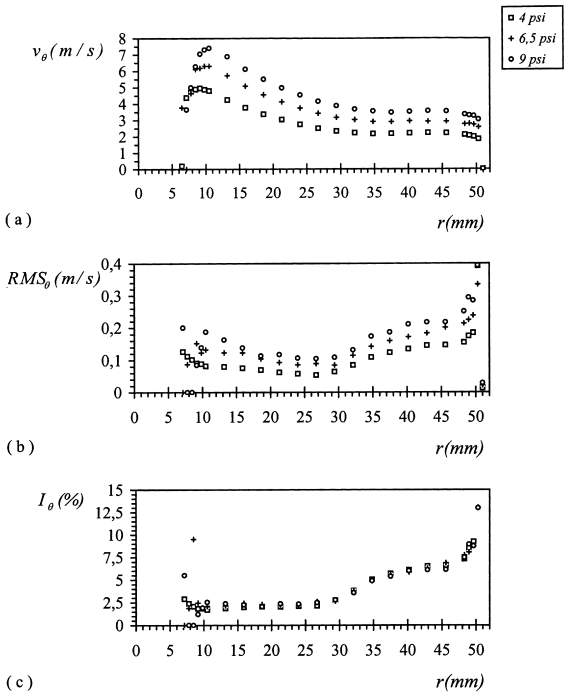

Fig. 6. Values of tangential velocity in the conical hydrocyclone: mean velocity, RMS values and turbulence intensity.

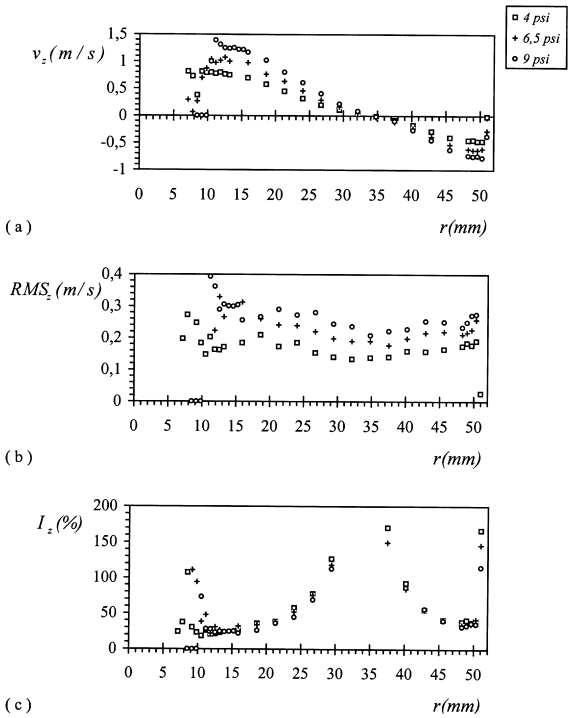

Fig. 7. Values of axial velocity in the cylindrical hydrocyclone: mean velocity, RMS values and turbulence intensity.

3.2. Flow in the cylindrical hydrocyclone

For the cylindrical hydrocyclone the experimental measurements show that, for each value of θ, $v_{z,M}$ increases with Δp and decreases linearly with z. The value of $v_{\theta,M}$ grows with Δp and it is virtually the same for changes in z. The radial coordinate of $v_{\theta,M}$ varies lightly through the vessel and moves radially outward when the feed pressure increases. A rise of Δp also produces a rise of $v_{z,m}$, which decreases continuously with the axial coordinate. The coordinate $r_{z,0}$ does not present any changes and is practically equal to 0.67 R for $z/H < 0.95$and to 0.77 R for $z/H \geq 0.95$.

In Fig. 7a–c the values of v_z, its RMS values and the intensity of turbulence are plotted for z=105 mm, θ=90° and Δp=4, 6.5, 9 while the tangential velocity data are given in Fig. 8a–c. In the same way as in the conical hydrocyclone, the RMS_z and RMS_θ are different since the velocity fluctuations are greater in the z direction. The RMS_θ maintains its minimum value just for $r = r_{z,0}$ but we observe higher RMS_z values in the flat bottom hydrocyclone. I_z and I_θ preserve the same profiles described for the conical hydrocyclone.

In the flat bottom hydrocyclone the axial movement of the fluid is completely different than in the conical vessel. Fig. 2a shows that v_z is approximately a linear function of z. For the flat bottom hydrocyclone the slope of the v_z curve decreases with z up to the bottom region where v_z is nearly zero, except near the air core where we find an upward flow. We have also verified that in the bottom region I_z is two order of magnitude greater than I_θ and that the turbulence

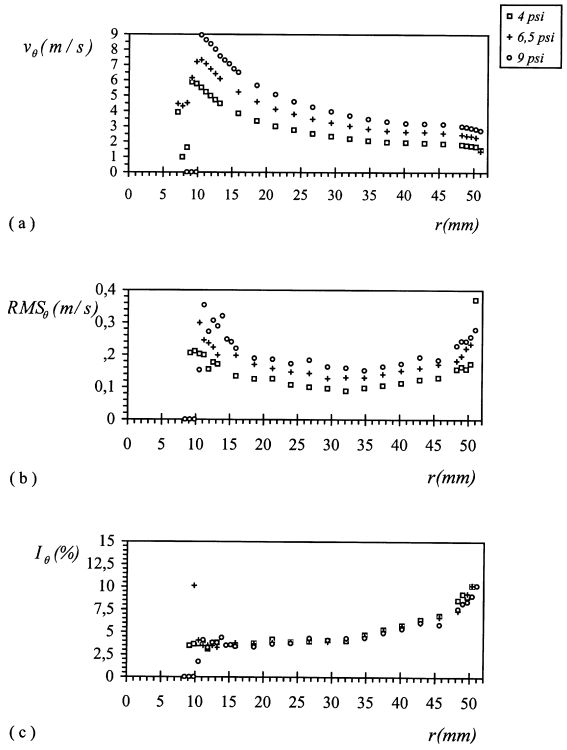

Fig. 8. Values of tangential velocity in the cylindrical hydrocyclone: mean velocity, RMS values and turbulence intensity.

in the conical hydrocyclone is higher than in the cylindrical vessel.

4. Conclusions

Three curved surfaces, the *solid wall*, the *mantle* and the *air core* bound the flow in the hydrocyclone. During the investigation the coordinate of the mantle $r_{z,0}$ was measured and it was observed that the coordinate $r_{\theta,M}$ of $v_{\theta,M}$ could be related to the air core position. We have noted that the distance between the air core surface and $r_{\theta,M}$ is approximately 2.5 mm for the conical vessel and 2 mm for the flat bottom hydrocyclone.

Our results have also shown that v_z in the conical hydrocyclone is lightly greater than in the cylindrical hydrocyclone. In this latter equipment v_z changes linearly with z up to the apex region, where the v_z profiles are completely different than in the conical hydrocyclone. Here, the axial velocity for the flat bottom hydrocyclone is the 20% of the axial velocity for the conical vessel. On the other hand the tangential velocity v_θ increases with Δp and presents the same general pattern in both hydrocyclones. In the cylindrical hydrocyclone v_θ does not practically change with the z coordinate.

Far from the solid wall and the air core surface, the values of the RMS_z and the RMS_θ are not the same in the two hydrocyclones. For z=105 mm and $0.2\ R \leq r \leq 0.7\ R$ the velocity fluctuations are higher in the flat bottom vessel while for intermediate z coordinates the RMS_z and the RMS_θ have similar magnitude in both hydrocyclones. Finally, the conical vessel shows greater turbulence intensity near the bottom discharge.

Acknowledgements

The authors acknowledge partial financial support of this work by the Fondef project D97-I2042. The present work is part of the M.Sc. thesis in Metallurgical Engineering of the first author at the University of Concepción, Chile.

References

[1] N. Bank, W.H. Gauvin, Measurement of flow characteristics in a confined vortex flow, Can. J. Chem. Eng. 55 (1977) 397–402.
[2] D.F. Kelsall, A study of the motion of solid particles in a hydraulic cyclone, Trans. Instn. Chem. Eng. 30 (1952) 87–108.
[3] G. Fanglu, L. Wenzhen, Measurement and study of velocity field in various cyclones by use of laser doppler anemometry, Proceeding of the Third International Conference on Hydrocyclones, Oxford, England, September to October 1987, pp. 65–74.
[4] K.T. Hsieh, R.K Rajamani, Mathematical model of the hydrocyclone based on physics of fluid flow, AIChE J. 37 (5) (1991) 735–746.
[5] P. Schummer, P. Noe, M. Baker, LDV measurements in the vortex flow created by a rotating wall dewatering cyclone, in: L. Svarovsky, M.T. Thew (Eds.), Hydrocyclones — Analysis and Applications, Kluwer, 1992, pp. 359–376.
[6] D. Baranov, A.M. Kutepov, I.G Ternovskii, Flow rate characteristics and hydrodynamics of a counterflow cylindrical hydrocyclone, J. Appl. Chem. — USSR (English trad.) 57 (5) (1984) 1181–1184.
[7] B. Chiné, F. Concha, G. Ferrara, LDA measurements of axial and tangential velocity components in a DMS cylindrical cyclone, Proceedings of the Eight International Symposium on Applications of Laser Techniques to Fluid Mechanics, Lisbon, Portugal, 8–11 July 1996, pp. 19.6.1.–19.6.6.
[8] F. Durst, A. Melling, J.H. Whitelaw, Principles and Practice of Laser Doppler Anemometry, Academic Press, London, 1981, pp. 342–346.
[9] B. Chiné, Experimental Study of the Swirling Flow in Hydrocyclones (in Spanish), MSc. Thesis, Department of Metallurgical Engineering, University of Concepción, Chile (1999).